COMMUNICATION TO THE EDITOR

BIOTECHNOLOGY and BIOENGINEERING

An Improved Dynamic Method to Measure k_La in Bioreactors

Andrew L. Damiani, Min Hea Kim, Jin Wang

Auburn University, 212 Ross Hall, Auburn, Alabama 36849; telephone: 1-334-844-2020; fax: 1-334-844-2063; e-mail: wang@auburn.edu

ABSTRACT: An accurate measurement or estimation of the volumetric mass transfer coefficient k_La is crucial for the design, operation, and scale up of bioreactors. Among different physical and chemical methods, the classical dynamic method is the most widely applied method to simultaneously estimate both k_La and cell's oxygen utilization rate. Despite several important follow-up articles to improve the original dynamic method, some limitations exist that make the classical dynamic method less effective under certain conditions. For example, for the case of high cell density with moderate agitation, the dissolved oxygen concentration barely increases during the re-gassing step of the classical dynamic method, which makes k_La estimation impossible. To address these limitations, in this work we present an improved dynamic method that consists of both an improved model and an improved procedure. The improved model takes into account the mass transfer between the headspace and the broth; in addition, nitrogen is bubbled through the broth when air is shut off. The improved method not only enables a faster and more accurate estimation of k_La, but also allows the measurement of k_La for high cell density with medium/low agitation that is impossible with the classical dynamic method. *Scheffersomyces stipitis* was used as the model system to demonstrate the effectiveness of the improved method; in addition, experiments were conducted to examine the effect of cell density and agitation speed on k_La.

Biotechnol. Bioeng. 2014;9999: 1–6.

KEYWORDS: oxygen transfer rate; k_La; dynamic method; oxygen utilization rate; mass transfer; bioreactors

Correspondence to: J. Wang
Contract grant sponsor: USDA-AFRI
Contract grant number: 2010-65504-20358
Contract grant sponsor: Sun Grant
Contract grant number: 8500014161
Contract grant sponsor: NSF
Contract grant number: 1264861
Contract grant sponsor: NSF IGERT
Contract grant number: 1069004
Received 30 January 2014; Revision received 10 March 2014; Accepted 3 April 2014
Accepted manuscript online xx Month 2014;
Article first published online in Wiley Online Library (wileyonlinelibrary.com).
DOI 10.1002/bit.25258

The oxygen transfer rate (OTR) is a crucial parameter in aerobic and microaerobic processes, since it is often the rate-limiting factor due to the low solubility of the oxygen in the broth. Therefore, it is an essential parameter that needs to be accurately measured or estimated for the design, operation, and scale-up of bioreactors (Garcia-Ochoa and Gomez, 2009). The transfer of the oxygen from the gas bubbles into the cells can be divided into two steps: (1) from the gas phase into the liquid medium phase; (2) from the liquid medium into the cells (or the consumption of oxygen by the cells). The mass transfer rates of oxygen corresponding to these two steps are termed oxygen transfer rate (OTR) and oxygen uptake rate (OUR), respectively. The overall mass balance for the dissolved oxygen (DO) in the well-mixed liquid phase can be written as:

$$\frac{dC_L}{dt} = \mathrm{OTR} - \mathrm{OUR} \tag{1}$$

where C_L denotes the dissolved oxygen concentration in the liquid phase. Based on the two film model (Whitman, 1923) and Henry's law, the net mass transfer of oxygen from the gas bubble to the liquid (i.e., OTR) can be expressed as

$$\mathrm{OTR} = k_La(hC_B - C_L) \tag{2}$$

where C_B is the oxygen concentration in the gas phase, h is the Henry's constant for oxygen and k_La is the volumetric mass transfer coefficient. It has been well recognized that k_La can be affected by many factors including the fluid properties (e.g., density, diffusivity, and viscosity), the size of the bubbles, the system geometry, and operating conditions (e.g., stirring speed in a stirred tank) (Blanch and Clark, 1996; Bouaifi et al., 2001; Linek et al., 2004; Martin et al., 2008; Özbek and Gayik, 2001; Wu, 1995). Many different methods to measure k_La have been published, which can be divided into two groups, chemical method and physical method (Suresh et al., 2009). The chemical methods (Cooper et al., 1944) use chemical reactions to determine the OTR or k_La and are not applicable for direct measurement of OUR. The physical methods (Baird et al., 1993; Tobajas and

Garcia-Calvo, 2000) use gas analyzer, gas chromatography or oxygen probes to measure the gas composition and calculate the OTR and OUR at the same time. Among different methods, the classical dynamic method (Bandyopadhyay and Murphrey, 1967) has been widely used to simultaneously measure k_La and OUR for different fermentation systems.

$$\frac{dC_L}{dt} = k_La(hC_B - C_L) - \text{OUR} \quad (3)$$

The classical dynamic method is a simple and elegant means to measure k_La, which only requires a fast responding DO probe (Rao, 2009). The schematic illustration of the classical dynamic method is given in Figure 1a. By introducing a brief interruption in the oxygen supply to the bioreactor, the overall process can be divided into two steps: degassing and re-gassing. During the degassing process, air is shut off and dissolved oxygen is consumed by cells. By fitting a straight line to the trajectory of the DO concentration, −OUR is estimated as the slope of the straight line. During the re-gassing process, air is resumed to bubble through the fermentation broth. By fitting the trajectory of DO concentration to the following equation, k_La can be estimated.

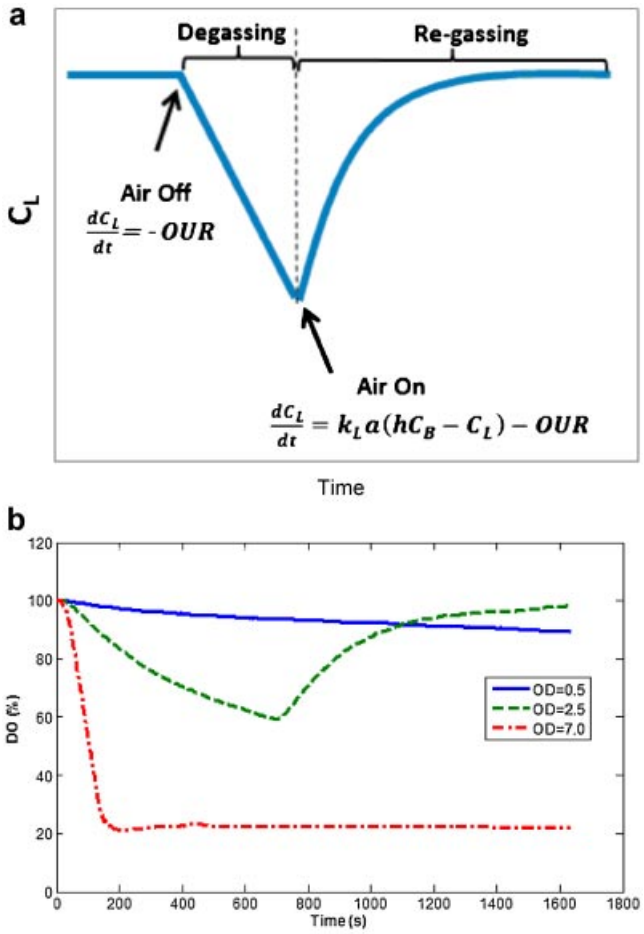

Figure 1. **a**: Schematic illustration of the classical dynamic method where OUR is estimated by fitting C_L to a straight line during the degassing process and OTR or k_La is estimated by fitting C_L to an exponential curve during the re-gassing process. **b**: Cases that the classical dynamic method are less effective in describing the dynamics of mass transfer: obvious curving trajectory during the degassing process ($OD_{600} = 2.5$); slow degassing process at low cell density ($OD_{600} = 0.5$); and slow re-gassing process at high cell density ($OD_{600} = 7.5$). Agitation speed was fixed at 350 rpm.

The classical dynamic method was rapidly adopted and became textbook material since its publication (Rao, 2009). In addition, several follow-up articles have been published over the years to improve the original method. In particular, the effect of the probe response time on the accuracy of the k_La measurement was studied by Heineken (1971). Despite many successful applications of the dynamic method to measure k_La for different bioprocesses, we had experienced some limitations during our experiments, which have not been addressed in the past. Some scenarios are described below and illustrated in Figure 1b.

(1) Curving DO trajectory during the degassing step: in our experiments conducted with yeast *Scheffersomyces stipitis*, the trajectory of the DO during the degassing process deviates from a straight line, which directly affects the estimation of OUR.
(2) Slow degassing process at low cell density: during our experiments of medium/high agitation with low cell density, DO decreases very slowly during the degassing step, which limits the range for the re-gassing step (i.e., $OD_{600} = 0.5$ in Fig. 1b). As a result, it is very difficult to obtain an accurate estimate of k_La due to the small perturbation introduced into the system, that is, the small change in the DO during the re-gassing step.
(3) Slow re-gassing process at high cell density: under the condition of high cell density with medium/low agitation when air is resumed after degassing step, the DO does not increase noticeably because of the high oxygen consumption rate, which makes the estimation of k_La very difficult (i.e., $OD_{600} = 7.0$ in Fig. 1b).

In addition, the mass transfer between the headspace and the liquid phase was not considered in the classical dynamic method, which could have significant impact under certain conditions as illustrated later. In this work, we present an improved dynamic method to address these limitations, which includes both an improved model and an improved procedure. In addition, we use *S. stipitis* as the model system to validate the proposed method, and to investigate the effects of cell concentration and agitation speed on k_La of the system.

To help understand the model development, different mass transfer components involved in an aerated bioreactor are illustrated in Figure 2. In the classical dynamic method, only mass transfer between the air bubbles and the liquid broth is considered. But in fact, mass transfer between the headspace

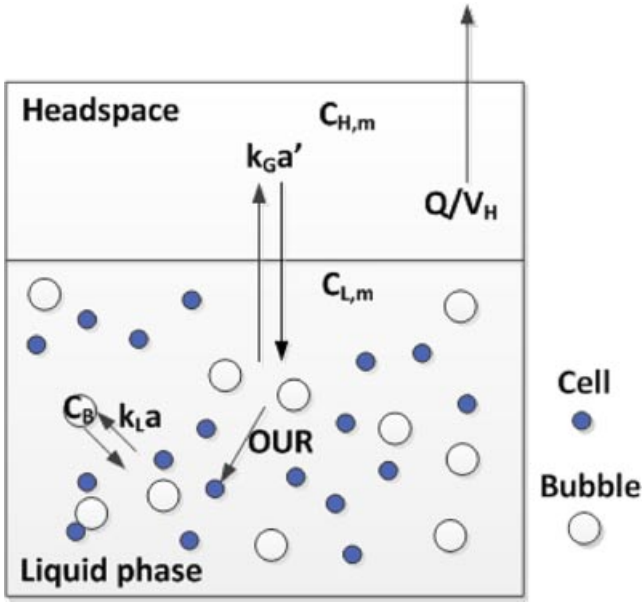

Figure 2. Schematic illustration of different mass transfer components involved in an aerated bioreactor.

and the liquid broth also exists, and sometimes may be dominant. To take this consideration into account, the total mass balance of the dissolved oxygen in a well-mixed liquid phase and headspace can be written as

$$\frac{dC_L}{dt} = k_La(hC_B - C_L) + k_Ga'(hC_H - C_L) - \text{OUR} \quad (4)$$

$$\frac{dC_H}{dt} = \frac{Q}{V_H}(C_B - C_H) - k_Ga'(hC_H - C_L) \quad (5)$$

where k_Ga' is the volumetric mass transfer coefficient between the headspace and the liquid phase; C_L, C_B, C_H, are the oxygen concentrations in liquid phase, bubbles, and headspace, respectively; Q is the volumetric flow rate of the air or nitrogen entering the headspace, V_H is the headspace volume. Because the measured DO during the experiments is always a relative concentration (i.e., percentage of the calibrated concentration), we convert the model into the relative concentration terms as follows:

$$\frac{dC_{L,m}}{dt} = k_La(C_{B,m} - C_{L,m}) + k_Ga'(C_{H,m} - C_{L,m}) - \text{OUR}^* \quad (6)$$

$$\frac{dC_{H,m}}{dt} = \frac{Q}{V_H}(C_{B,m} - C_{H,m}) - k_Ga'h(C_{H,m} - C_{L,m}) \quad (7)$$

where $\text{OUR}^* = \text{OUR}/hC_0$; $C_{L,m} = C_L/hC_0$ and $C_{H,m} = C_H/C_0$, are the measured relative DO concentrations in the liquid phase and headspace, respectively, with the DO probe calibrated by the air (or diluted air) fed to the bioreactor (C_0).

Compared to the classical dynamic method, the major difference of the modified method is that: during the degassing step, instead of simply shutting off the air supply, we replace air (or diluted air) with nitrogen of the same flow rate, which speeds up the descending process of DO, sometimes significantly; then in the re-gassing step, nitrogen is switched to air (or diluted air) of the same flow rate to bring the DO up. For the improved method, we introduce the following terminology changes. During the "degassing" step, because of the continuous supply of the nitrogen gas instead of complete shutoff of air supply, we rename this step "desorption process," as the gas–liquid mass transfer will result in the desorption of DO into nitrogen bubbles. Correspondingly, for the "re-gassing" step, we rename it "absorption process." There are several important benefits of the improved procedure. First, it allows a low DO level to be achieved quickly during the desorption process, which not only greatly reduces the risk that the cells could transit into different physiological states during the process, but also allows a larger DO change during the absorption process. As noted earlier, a larger change in DO during the absorption process is desirable, as it can improve the accuracy of the estimated k_La. Second and more importantly, for the case of high cell density where the DO does not increase noticeably during the absorption process, k_La can be estimated based on the descending DO curve obtained during the desorption process alone. Note that in order to do so, we assume that the air-liquid and nitrogen-liquid interfaces (i.e., A_{air} and A_{N_2}) are the same. This is reasonable as O_2 and N_2 have similar physical properties, and about 80% of air is N_2 anyway. In addition, this assumption was supported by our experiments.

It should be noted that the mass transfer between the headspace and the liquid phase was considered in Muller et al. (2012), which also considered the change of C_B. Strictly speaking, C_B keeps decreasing as the bubbles travel through the liquid phase due to the mass transfer. However, because of the short residence time in our experiments and most bioreactors, the amount of the oxygen transferred into the liquid phase is very limited—less than 5% even for the condition of the highest k_La for our experiments. Therefore, C_B is assumed constant in this work ($C_B = 0$ during the desorption process and $C_B = C_0$ during the absorption process). In addition, we did not consider the probe response time, mainly because the dynamics of the system (with time constant 30–40 min) is much slower than the dynamics of the probe (with time constant about 40 s).

For the modified dynamic procedure described above, during the desorption process, because $C_{B,m} = 0$, Equations (6) and (7) can be simplified as follows:

$$\frac{dC_{L,m}}{dt} = -k_LaC_{L,m} + k_Ga'(C_{H,m} - C_{L,m}) - \text{OUR}^* \quad (8)$$

$$\frac{dC_{H,m}}{dt} = -\frac{Q}{V_H}C_{H,m} - k_Ga'h(C_{H,m} - C_{L,m}) \quad (9)$$

During the absorption process, because we assume $C_B = C_0$ (or $C_{B,m} = 1$), Equations (6) and (7) can be simplified as follows:

$$\frac{dC_{L,m}}{dt} = k_L a(1 - C_{L,m}) + k_G a'(C_{H,m} - C_{L,m}) - OUR^* \quad (10)$$

$$\frac{dC_{H,m}}{dt} = \frac{Q}{V_H}(1 - C_{H,m}) - k_G a' h(C_{H,m} - C_{L,m}) \quad (11)$$

It is worth noting that fitting either $C_{L,m}$ or $C_{H,m}$ during the desorption or absorption processes (i.e., any one of the analytical solutions of the Equations (8)–(11) provided in Supplemental Information) allows us to estimate OUR*, $k_L a$ and $k_G a'$, simultaneously. Therefore, if both $C_{L,m}$ and $C_{H,m}$ are available over both desorption and absorption processes, we can obtain four sets of independently estimated parameters based on Equations (8)–(11), and the consistency among them can serve as an indicator of the accuracy of the estimated parameters.

Experiments were conducted to demonstrate the effectiveness of the proposed method, Four cases of different cell density ($OD_{600} = 1.5, 3.0, 4.5, 10.0$) at fixed agitation speed of 450 rpm were examined. Three replicates were conducted for each case. Figure 3 shows one case ($OD_{600} = 4.5$) of the measured $C_{L,m}$ and $C_{H,m}$, as well as the predictions generated by the fitted models. Both $C_{L,m}$ and $C_{H,m}$ of the three replicates are very close to each other. To reduce clutter, the measurements and predictions of the replicate 2 were shifted up by 0.2, and the replicate 3 by 0.4. From Figure 3 it is observed that the model predictions agree with the measurements very well, which indicates that the models capture the dominant dynamics of the mass transfer processes well for both $C_{L,m}$ and $C_{H,m}$, during both desorption and absorption processes. In addition, it indicates that assuming C_B as a constant does not introduce noticeable error to the model. The estimated model parameters are listed in Table I together with the other three cases. For all four cases, the estimated parameters from the three replicates are almost identical; therefore no standard deviation was provided in the table. It is worth noting that the four estimates of the parameters, obtained independently from $C_{L,m}$ during desorption, $C_{L,m}$ during absorption, $C_{H,m}$ during desorption and $C_{H,m}$ during absorption independently, agree with each other well, which not only confirms that using nitrogen bubbles to estimate the $k_L a$ is feasible, but also offers further validation of the accuracy of the estimated $k_L a$. This offers a significant advantage over the classical dynamic method for a couple of reasons. Because the process of fitting solutions of Equations (8)–(11) with measurements is a nonlinear optimization process, there always exist multiple local solutions. How to pick the correct one is nontrivial due to the nonlinearity of the optimization problem, as the set of parameters that give the smallest fitting error are often not the true parameters. With multiple independent ways to estimate the parameters, such as through $C_{L,m}$ during desorption and absorption, or $C_{H,m}$ and $C_{L,m}$ during desorption, it allows us to find the correct parameters relatively easily, because only the set of true parameters could minimize the fitting error of multiple objective functions. The analytical solutions to the model equations (i.e., Equations (8)–(11)) and corresponding codes for the curve fitting process can be found in Supplemental Information.

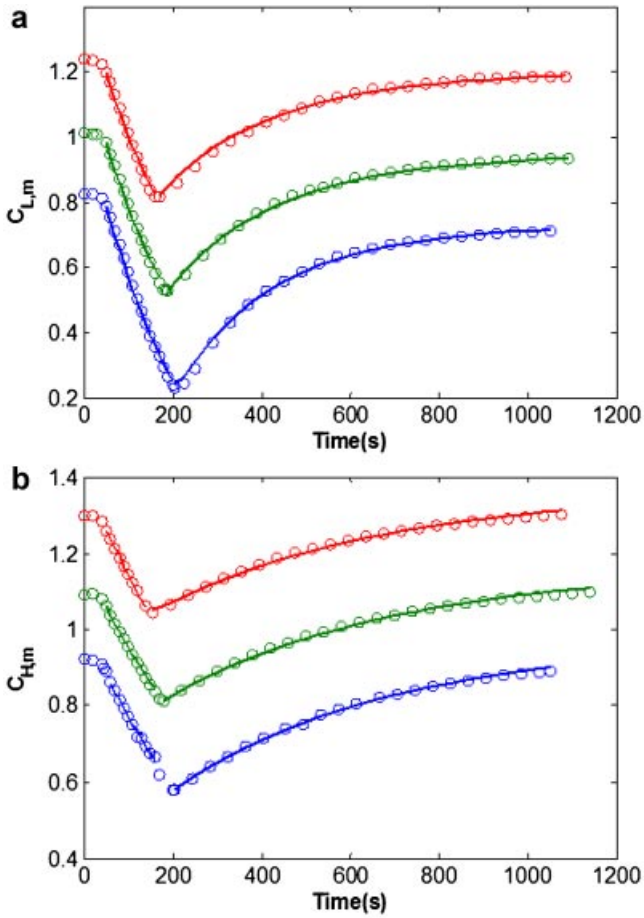

Figure 3. Experimental measurements and predictions from the fitted models of three replicates at $OD_{600} = 4.5$ and agitation speed of 450 rpm. **a**: Liquid phase; (**b**) headspace. To reduce clutter, the measurements (green circles) and predictions (green lines) of replicate 2 were shifted up by 0.2, and replicate 3 (red circles and lines) were shifted up by 0.4. Without shifting, the three replicates overlap each other.

Three replicates of the experiments were conducted to examine the effects of cell density (OD_{600}) and agitation speed (rpm) on $k_L a$ and OUR for the system with *S. stipitis*. For cell density, five different OD_{600} were studied, which are 0, 1.5, 3.0, 4.5, and 10.0. For agitation speed, three conditions were studied, which are 250, 350, and 450 rpm. The results are shown in Figure 4 where Figure 4a shows the estimated parameters obtained from the model as a function of agitation speed for $OD_{600} = 3.0$, and Figure 4b shows the estimated parameters obtained from the model as a function of OD_{600} for the agitation speed of 350 rpm. From Figure 4a, it can be seen that both $k_L a$ and $k_G a'$ increase with increasing agitation speed due to the increase of interfacial area of

Table I. Estimated model parameters of different cases (various OD_{600} at the fixed agitation speed of 450 rpm).

	450 rpm			
	From C_L		From C_H	
Parameter (10^{-3} s^{-1})	Desorption	Absorption	Desorption	Absorption
$OD_{600} = 1.5$				
k_La	5.55	5.55	5.54	5.55
k_Ga'	9.01	9.01	9.00	9.00
OUR*	7.01	7.01	7.00	7.00
$OD_{600} = 3.0$				
k_La	6.00	6.02	6.02	6.01
k_Ga'	9.25	9.24	9.21	9.25
OUR*	6.31	6.32	6.25	6.70
$OD_{600} = 4.5$				
k_La	4.11	4.12	4.11	4.12
k_Ga'	9.22	9.22	9.20	9.11
OUR*	1.81	1.85	1.87	1.87
$OD_{600} = 10.0$				
k_La	3.64	3.77	3.71	3.85
k_Ga'	1.21	1.11	1.23	1.10
OUR*	1.32	1.42	1.47	1.67

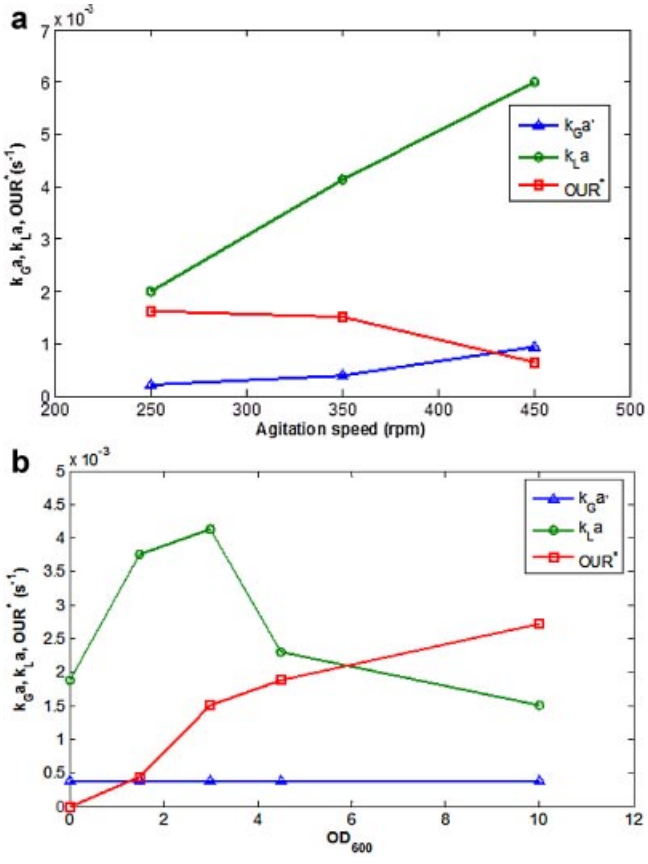

Figure 4. Effect of cell density and agitation speed on k_La, k_Ga', and OUR*: (**a**) effect of agitation speed at $OD_{600} = 3.0$; (**b**) effect of cell density at agitation speed of 350 rpm.

bubble-liquid and headspace-liquid, with k_La increases much faster than k_Ga'; while OUR* decreases with increasing agitation speed, which can be explained by the physical blocking effect (Ju and Sundararajan, 1995). From Figure 4b, it is observed that k_Ga' is not affected by the cell density. This is expected because at the same agitation speed, the interfacial area between headspace and liquid phase is not affected by cell density, therefore k_Ga' is not affected by cell density. In addition, OUR* increases with cell concentration in a nonlinear fashion, which has been observed somewhere else (Garcia-Ochoa et al., 2010). Finally, with increasing cell density, k_La first increases and reaches a maximum then subsequently decreases. This phenomenon can be explained by the overall result of several mechanisms. At low cell density, the dominant factor that affects k_La is the surface renewal and modification of medium by the cells, which results in increased specific gas–liquid interfacial area and k_La (Ju and Sundararajan, 1995); while at high cell density, cells' blocking effect and absorption of cells to the bubble-liquid interface result in decreased specific interfacial area and less distribution of bubbles, therefore decreased k_La (Galaction et al., 2004; Martin et al., 2010).

In summary, the improved dynamic method is shown to be simple and effective in obtaining k_La, in a faster and more accurate way than the classical dynamic method. It can utilize the desorption process alone to obtain estimates on k_La, k_Ga, and OUR. In addition, our experiments on *S. stipitis* confirm that the presence of microorganisms can affect k_La significantly, with enhanced k_La at low cell density, and reduced k_La at high cell density. It is worth noting that dynamic methods (both the classical one and the improved one) estimate OUR based on the mass balance of the liquid space (and head space), while measuring OUR through mass spectrometry monitoring systems adhere to performing a global mass balance. Therefore, depending on what is the rate limiting step (either OUR or OTR), the OUR obtained from the mass spec method could be the same or different from that obtained from the dynamic methods. When OTR is smaller than OUR, how much oxygen the cells can consume is limited by OTR and DO is closed to 0. Under this condition, OUR obtained from the dynamic method would be large than the OUR obtained from mass spec, and the amount of the oxygen consumed by the cells should be calculated from OTR (i.e., via k_La and k_Ga'), instead of the measured OUR. If OTR is larger than OUR, DO will be larger than 0, then the OUR obtained from mass spec monitoring system and the dynamic method would be the same. Although a mass spec monitoring system always obtains the actual amount of oxygen that the cells consumed, it has its own limitations. For example, the instrumentation needs to be highly accurate, since the measurements of the inlet and outlet compositions usually are different only slightly in the case of low OUR, which is quite often. Also the mass spec method requires that the DO be constant in order to attain accurate results, where it was recommended to keep DO from changing $\pm 0.05\%$. On the other hand, the limitation of the dynamic methods is that the physiochemical

change of the media and physiological changes in the cells could be introduced because of the required perturbation.

Materials and Methods

S. stipitis CBS5773 cells were pre-cultured in minimal medium containing (per liter) 20 g D-xylose, 1.7 g yeast nitrogen base without amino acids or ammonium sulfate and 2.27 g urea. Culture medium used in all experiments contained (per liter) 0.5 g D-xylose, 1.7 g yeast nitrogen base without amino acids or ammonium sulfate and 2.27 g urea. All experiments were conducted in a New Brunswick BioFlo110 fermenter (3 L) with a working volume of 1.5 L under sterile condition. The DO concentrations in the liquid and headspace were monitored with polarographic dissolved oxygen electrodes Inpro6800 (Mettler-Toledo, Columbus, OH). Air or nitrogen gas was used as the gas phase for re-gassing or absorption and degassing or desorption respectively, in all the experiments. The gas flow rate was kept constant at 196 mL/min. Experiments were performed with various agitation speeds (250, 350, 450 rpm) and biomass concentrations ($OD_{600} = 0.0$, 1.5, 3.0, 4.5, 10.0).

The authors declare no conflict of interest. This work was funded by USDA-AFRI (2010-65504-20358), Sun Grant (8500014161), NSF (1264861), and NSF IGERT (1069004). The authors thank Dr. Q. Peter He for providing valuable comments and suggestions on this work.

References

Baird MHI, Rama NV, Shen ZJ. 1993. Oxygen absorption in a baffled tank agitated by delta paddle impeller. Can J Chem Eng 71:195–201.

Bandyopadhyay B, Murphrey AE. 1967. Dynamic measurement of the volumetric oxygen transfer coefficient in fermentation systems. Biotechnol Bioeng 15:533–544.

Blanch HW, Clark DS. 1996. Biochemical Engineering, Marcel Dekker Inc.

Bouaifi M, Hebrard G, Bastoul D, Roustan M. 2001. A comparative study of gas hold-up, bubble size, interfacial area and mass transfer coefficients in stirred gas–liquid reactors and bubble columns. Chem Eng Proc 40:97–111.

Cooper CM, Fernstorm GA, Miller SA. 1944. Performance of agitated gas–liquid contactors. Ind Eng Chem 6:504–509.

Galaction AI, Cascaval D, Oniscu C, Turnea M. 2004. Prediction of oxygen mass transfer coefficients in stirred bioreactors for bacteria, yeasts and fungus broths. Biochem Eng J 20:85–94.

Garcia-Ochoa F, Gomez E. 2009. Bioreactor scale-up and oxygen transfer rate in microbial processes: An overview. Biotechnol Adv 27:153–176.

Garcia-Ochoa F, Gomez E, Santos V, Merchuk JC. 2010. Oxygen uptake rate in microbial processes: An overview. Biochem Eng J 49:289–307.

Heineken FG. 1971. Oxygen mass transfer and oxygen respiration rate measurements utilizing fast response oxygen electrodes. Biotechnol Bioeng 84:351–358.

Ju LK, Sundararajan A. 1995. The effects of cells on oxygen transfer in bioreactors. Bioprocess Eng 13, 271–278.

Linek V, Kordac M, Fujasova M, Moucha T. 2004. Gas–liquid mass transfer coefficient in stirred tanks interpreted through models of idealized eddy structure of turbulence in the bubble vicinity. Chem Eng Proc 43:1511–1517.

Martin M, Montes FJ, Galan MA. 2008. Bubbling process in stirred tank reactors II: Agitator effect on the mass transfer rates. Chem Eng Sci 63:3223–3234.

Martin M, Montes FJ, Galan MA. 2010. Mass transfer rates from bubbles in stirred tanks operating with viscous fluids. Chem Eng Sci 65:3814-3824.

Muller S, Murray DB, Machne R. 2012. A new dynamic model for highly efficient mass transfer in aerated bioreactors and consequences for k_La identification. Biotechnol Bioeng 109:2997–3006.

Özbek B, Gayik S. 2001. The studies on the oxygen mass transfer coefficient in a bioreactor. Proc Biochem 36:729–741.

Rao G. 2009. Vintage paper: Dynamic measurement of the volumetric oxygen transfer coefficient in fermentation systems. Biotechnol Bioeng 104:841–852.

Suresh S, Srivastava VS, Mishra IM. 2009. Techniques for oxygen transfer measurement in bioreactors: A review. J Chem Technol Biotechnol 84:1091–1103.

Tobajas M, Garcia-Calvo E. 2000. Comparison of experimental methods for determination of the volumetric mass transfer coefficient in fermentation processes. Heat Mass Transfer 36:201–207.

Whitman WG. 1923. Preliminary experimental confirmation of the two-film theory of gas absorption. Chem Metall Eng 29:146–149.

Wu H. 1995. An issue on applications of a disk turbine for gas–liquid mass transfer. Chem Eng Sci 50:2801–2811.

Supporting Information

Additional supporting information may be found in the online version of this article at the publisher's web-site.